

# Structural connectivity of right frontal hyperactive areas scales with stuttering severity

Nicole E. Neef,<sup>1,2</sup> Alfred Anwander,<sup>1</sup> Christoph Bütfering,<sup>2</sup> Carsten Schmidt-Samoa,<sup>3</sup> Angela D. Friederici,<sup>1</sup> Walter Paulus<sup>2</sup> and Martin Sommer<sup>2</sup>

A neuronal sign of persistent developmental stuttering is the magnified coactivation of right frontal brain regions during speech production. Whether and how stuttering severity relates to the connection strength of these hyperactive right frontal areas to other brain areas is an open question. Scrutinizing such brain–behaviour and structure–function relationships aims at disentangling suspected underlying neuronal mechanisms of stuttering. Here, we acquired diffusion-weighted and functional images from 31 adults who stutter and 34 matched control participants. Using a newly developed structural connectivity measure, we calculated voxel-wise correlations between connection strength and stuttering severity within tract volumes that originated from functionally hyperactive right frontal regions. Correlation analyses revealed that with increasing speech motor deficits the connection strength increased in the right frontal aslant tract, the right anterior thalamic radiation, and in U-shaped projections underneath the right precentral sulcus. In contrast, with decreasing speech motor deficits connection strength increased in the right uncinate fasciculus. Additional group comparisons of whole-brain white matter skeletons replicated the previously reported reduction of fractional anisotropy in the left and right superior longitudinal fasciculus as well as at the junction of right frontal aslant tract and right superior longitudinal fasciculus in adults who stutter compared to control participants. Overall, our investigation suggests that right fronto-temporal networks play a compensatory role as a fluency enhancing mechanism. In contrast, the increased connection strength within subcortical-cortical pathways may be implied in an overly active global response suppression mechanism in stuttering. Altogether, this combined functional MRI–diffusion tensor imaging study disentangles different networks involved in the neuronal underpinnings of the speech motor deficit in persistent developmental stuttering.

1 Department of Neuropsychology, Max Planck Institute for Human Cognitive and Brain Sciences, Leipzig, Germany

2 Department of Clinical Neurophysiology, University Medical Center Göttingen, Göttingen, Germany

3 Department of Cognitive Neurology, University Medical Center Göttingen, Germany

Correspondence to: Dr Nicole E. Neef

Department of Neuropsychology

Max Planck Institute for Human Cognitive and Brain Sciences

Stephanstraße 1a, 04103 Leipzig, Germany

E-mail: nneef@gwdg.de

**Keywords:** persistent developmental stuttering; diffusion tractography; connection strength; right frontal networks; speech motor control

**Abbreviations:** DTI = diffusion tensor imaging; FAT = frontal aslant tract; IFG = inferior frontal gyrus; MFG = middle frontal gyrus; OASES = overall assessment of stuttering the speakers experience of stuttering; SLF = superior longitudinal fasciculus; SMA = supplementary motor area; SSI-4 = stuttering severity instrument; TBSS = tract-based spatial statistics

Received February 22, 2017. Revised September 26, 2017. Accepted October 11, 2017. Advance Access publication December 8, 2017

© The Author (2017). Published by Oxford University Press on behalf of the Guarantors of Brain.

This is an Open Access article distributed under the terms of the Creative Commons Attribution Non-Commercial License (<http://creativecommons.org/licenses/by-nc/4.0/>), which permits non-commercial re-use, distribution, and reproduction in any medium, provided the original work is properly cited. For commercial re-use, please contact [journals.permissions@oup.com](mailto:journals.permissions@oup.com)

## Introduction

Persistent stuttering is a fluency disorder that occurs during early childhood without obvious reason and persists in ~1% of the adult population, predominantly in males (Yairi and Ambrose, 1999, 2013). Characteristic signs are involuntary sound and syllable repetitions, sound prolongations, and speech blocks (Bloodstein and Ratner, 2008). Dysfluencies are frequently accompanied by facial grimacing, head and limb movements. Furthermore, negative emotions and avoidance behaviour accompany stuttering (Iverach and Rapee, 2014). Depending on severity, persistent stuttering seriously compromises quality of life (Koedoot *et al.*, 2011).

Fluent speech production relies on the dynamic organization of large-scale brain networks that coordinate cognitive, sensorimotor, and emotional systems. Reliable connectivity and effective signal transfer are essential to converge and convey speech, but involved brain regions show atypical activity in persistent developmental stuttering (Fox *et al.*, 1996; De Nil *et al.*, 2000; Salmelin *et al.*, 2000; Neumann *et al.*, 2003; Lu *et al.*, 2010; Toyomura *et al.*, 2011; Craig-McQuaide *et al.*, 2014; Etchell *et al.*, 2014). Atypical activation patterns vary with imaging method and paradigm (Ingham *et al.*, 2012) as well as with the neural signatures left by lifelong experience of stuttering and diverse therapies (Wymbs *et al.*, 2013). One of the most robust neural signatures of stuttering is an excessive recruitment of right frontal cortical areas while speaking. Right primary motor cortex, premotor cortex, supplementary motor area (SMA), pre-SMA, inferior frontal gyrus (IFG), insula, frontal and the rolandic operculum show amplified speech-related activity (Budde *et al.*, 2014; Belyk *et al.*, 2015), with most robust evidence for right rolandic operculum and precentral gyrus [Brodmann area (BA) 4/6, Belyk *et al.*, 2017]. Previous studies discuss whether right frontal hyperactivations are related to compensatory, causal, or maladaptive mechanisms (Fox *et al.*, 2000; Neumann *et al.*, 2003; Preibisch *et al.*, 2003; Watkins *et al.*, 2008; Chang *et al.*, 2009; Kell *et al.*, 2009; Neef *et al.*, 2011, 2016). To separate these mechanisms several studies correlated local brain activity with stuttering severity. Negative correlations have been taken to suggest a compensatory role of the right frontal operculum (Preibisch *et al.*, 2003; Kell *et al.*, 2009). Positive correlations were reported for activity in the right primary motor cortex (Fox *et al.*, 2000; Chang *et al.*, 2009), right SMA, and right anterior insula (Fox *et al.*, 2000). However, cross-sectional studies of the adult brain do not allow a distinction between causal factors that are associated with the risk of developing stuttering, and maladaptation, which is a result of life-long stuttering. Thus, right frontal regions show both signs of compensatory activity and signs of causal or maladaptive activity.

We still lack a clear understanding of supposed compensatory or causal mechanisms. Our previous functional MRI study, in which we propose a potential neuropathological

principle, showed that right IFG activity relates to the inhibition of speech responses (Neef *et al.*, 2016). We propose that stuttering might be caused by an overly active global response suppression mechanism mediated via the subthalamic nucleus-right IFG-basal ganglia hyperdirect pathway. An amplified involvement of the hyperdirect pathway might increase the system's tendency to globally inhibit motor responses. Fast inhibition via the hyperdirect pathway is unspecific and induces a global reduction of the thalamo-cortical drive (Nambu *et al.*, 2002; Aron, 2011; Aron *et al.*, 2014). If this global inhibition is too strong or imbalanced, as proposed in stuttering, the stopping of an ongoing speech motor programme and/or the selection of a succeeding speech motor programme might fail. Such a failure would lead to sound prolongations, sound repetitions and blocking of speech as characteristic for stuttering. An overly involved hyperdirect pathway might exhibit an increased structural connectivity within the larger network. Connections between right hemisphere IFG, pre-SMA, subthalamic nucleus, and striatum are the structures of interest already suggested by neuroimaging evidence (Aron and Poldrack, 2006; Aron *et al.*, 2007; Jahanshahi *et al.*, 2015). Here, we investigate white matter structures that connect right frontal hyperactive regions with the rest of the brain, in order to test whether connection properties support our proposed hypothesis, specifically that stuttering might be related to an irregular global response suppression mediated via the hyperdirect pathway.

Diffusion-weighted MRI quantifies properties of white matter structures and, thus, helps to scrutinize structural connectivity. In the context of stuttering, a number of diffusion-weighted MRI studies report a reduced fractional anisotropy in speech-related fibre pathways, such as the left superior longitudinal fasciculus (SLF; Sommer *et al.*, 2002; Chang *et al.*, 2008; Watkins *et al.*, 2008; Kell *et al.*, 2009; Cykowski *et al.*, 2010; Cai *et al.*, 2014a; Kronfeld-Duenias *et al.*, 2016b), a prominent dorsal fibre pathway that includes the arcuate fasciculus (Makris *et al.*, 2005) and that connects fronto-parieto-temporal regions (Catani *et al.*, 2005) of the speech network (Hickok and Poeppel, 2007). More recently, structural differences were also shown in the left frontal aslant tract (FAT; Kronfeld-Duenias *et al.*, 2016a), a fibre pathway that connects the posterior region of the IFG with the SMA and pre-SMA (Catani *et al.*, 2012), relevant for fluent speech production (Guenther, 2016; Kemerdere *et al.*, 2016). However, the picture that emerges from previous diffusion-weighted MRI studies on stuttering is diffuse (Neef *et al.*, 2015). Although only a few findings have been replicated, these jointly highlight the implication of left hemisphere speech-related fibre paths. Reports on right hemisphere white matter differences are less robust (Cai *et al.*, 2014a; Neef *et al.*, 2015). For the frontal lobe, structural differences are reported in the white matter underneath the IFG, premotor cortex, and middle frontal gyrus (MFG; Watkins *et al.*, 2008; Connally *et al.*, 2014; Chang *et al.*, 2015), in the anterior segment of the right anterior fasciculus

(Kronfeld-Duenias *et al.*, 2016b), and in the right FAT (Kronfeld-Duenias *et al.*, 2016a).

Inconsistency among white matter findings can partly be explained by the variety of analysis approaches used. White matter differences in stuttering resulted from voxel-based statistics (Sommer *et al.*, 2002), region of interest-based analysis (Chang *et al.*, 2008), or tract-based spatial statistics (TBSS; Watkins *et al.*, 2008; Kell *et al.*, 2009; Cykowski *et al.*, 2010; Cai *et al.*, 2014a; Connally *et al.*, 2014; Chang *et al.*, 2015; Civier *et al.*, 2015). Fewer studies used fibre tracking methods to scrutinize structural connectivity (Chang *et al.*, 2011; Cai *et al.*, 2014a; Connally *et al.*, 2014; Cieslak *et al.*, 2015). The former methods locate microstructural changes at specific points in the white matter, while the latter mainly characterize the probability and strength of connection between any two points in the brain (Morris *et al.*, 2008). Hybrid approaches locate microstructural white matter differences within such a connecting volume (Kronfeld-Duenias *et al.*, 2016a, b).

As a major difference to previous diffusion tensor imaging (DTI) studies on stuttering, we used a different approach to test structural connectivity. To enable comparison with most previous studies we also calculated TBSS. This first step helped with locating microstructural differences in the white matter skeleton, when comparing adults who stutter and fluent control speakers. In a second step we fed TBSS seeds into probabilistic tractographies to generate connection probability density maps (Behrens *et al.*, 2003, 2007) and to reconstruct involved fibre pathways within and between both hemispheres. This procedure allowed us to determine fibre pathways that are affected in stuttering. Furthermore, a larger brain network that is involved in stuttering was derived by this procedure. In a third step, we combined DTI-based probabilistic fibre tracking and functional MRI to gain probability density maps of right frontal hyperactive cortical regions in adults who stutter. Eventually, in a fourth step, we used these probability density maps to determine space and volume for correlation analyses between the connection probability density of each voxel and stuttering severity. In this context, a significant cluster reflects the likelihood and the relative connection density, a seed region shows with this white matter region when related to stuttering severity. For the sake of simplicity, we use the term connection strength to refer to connection probability density.

In this study, we combined TBSS, DTI-based probabilistic fibre tracking and functional MRI to determine white matter differences between adults who stutter and matched control participants, and to scrutinize how the structural connectivity of right frontal hyperactive areas relates to stuttering severity. Only a few studies combined both functional MRI and DTI to study the neuronal basis of stuttering (Watkins *et al.*, 2008; Kell *et al.*, 2009; Chang *et al.*, 2011), and only one study combined structural and functional connectivity analyses in the same subjects (Chang *et al.*, 2011). This latter study showed that both functional and structural connectivity of the left and right IFG pars

opercularis with their ipsilateral premotor and motor regions were decreased in the left hemisphere, but tended to be increased in the right hemisphere in adults who stutter compared to fluent speakers. Until today, no study investigated the link between right frontal hyperactivations, white matter connectivity, and stuttering severity within the right frontal lobe, examined here. In the context of our hypothesis that stuttering might be caused by an irregular global response suppression, such knowledge would make a good starting point for the rational design of brain stimulation approaches (Chesters *et al.*, 2017), because it would advise the appropriate site and direction (inhibitory or excitatory) of potential stimulation protocols.

## Materials and methods

### Participants

Participants were recruited for an MRI study that tested sex differences in persistent developmental stuttering (Bütfering, 2015). Here we included only participants that successfully finished functional MRI scanning and diffusion-weighted MRI scanning, of which 31 participants were adults who stutter (15 females, aged 19–63 years, median age 36.0 years, SD = 12.3) and 34 participants were matched controls (17 females, 20–62 years, median age 35.5 years, SD = 12.3). Participants reported no neurological impairment, drug use, or medical history that might affect their brain structure or function. Twenty-two adults who stutter reported a family history of stuttering. None of the fluent speakers reported a family history of speech or language disorders. Groups were matched for age, sex, handedness (Oldfield, 1971), and years of formal education. Table 1 summarizes the demographic information of the participants. Individual characteristics of all participants are provided in Supplementary Tables 1 and 2. Approval from the local ethics committee at the University Medical Center, Göttingen, Germany, and written informed consent was obtained prior to the study. Each participant was paid €20 for participating.

**Table 1** Participants, demographic information, and behavioural results

	AWS	Control	P-value
<i>n</i>	31	34	n/a
Age in years (mean)	36.7 (12.3)	37.1 (12.7)	0.90 <sup>a</sup>
Sex (male) (%)	16 (52)	17 (50)	0.90 <sup>b</sup>
Handedness (mean LQ)	92.6 (11.5)	95.2 (8.5)	0.31 <sup>a</sup>
Education (median)	5	4	0.21 <sup>c</sup>
Age of stuttering onset (years)	4.3 (1.7)	n/a	n/a
SSI-4 total score (mean)	16.6 (11.5)	n/a	n/a
OASES total score (mean)	46.2 (12.0)	n/a	n/a

<sup>a</sup>T-test.

<sup>b</sup> $\chi^2$ -test.

<sup>c</sup>Mann-Whitney U-test.

AWS = adults who stutter; Education (1 = school; 2 = high school; 3 = <2 years university; 4 = 2 years university; 5 = 4 years university; 6 = postgraduate); n/a = not applicable.

According to the OASES (German version of the Overall Assessment of the Speakers Experience of Stuttering; Yaruss and Quesal, 2006), two adults who stutter estimated the total impact of stuttering on their life as mild, 10 as mild-to-moderate, 16 as moderate, one as moderate-to-severe, and one as severe. One adult who stutters refused to fill out the OASES from section 2 to 4, thus no total impact was reported. The stuttering severity instrument (SSI-4) (Riley, 2009) captures the frequency and duration of stuttered syllables as well as physical concomitants of stuttering. According to the SSI-4, eight participants showed very mild stuttering, seven were mild, two were moderate, two were severe, and two were very severe. Eight participants had an SSI score lower than 10, but were included in the analysis because they perceived themselves as persons who stutter as indicated by the OASES. There are two possible reasons for the underscores. First, all participants who stutter reported that they participated in stuttering therapy at least once in their life. Although, nobody was under treatment while participating in the current study, treatment experience made it possible that fluency-inducing techniques were used during the course of the interview. We tried to minimize this effect by explicitly asking our participants to allow stuttering. Second, all participants were recruited by the author C.B., who stutters himself and who knew the participants who stutter from various annual meetings organized across Germany by the German Stuttering Association. He did not participate in the current study because his handedness is left. All interviews were conducted by C.B. Because of the familiarity between the interviewer and the participants who stutter and because the interviewer is a person who stutters himself, speech samples were acquired in a relaxed situation. It is highly likely that these circumstances led to an enhanced fluency and thus to an underestimation of stuttering severity.

## Image acquisition

MRI was conducted in a 3-T scanner (Tim Trio, Siemens Healthineers) using an 8-channel head coil for signal reception. Initially, structural whole-brain  $T_1$ -weighted MRI were recorded using a non-selective inversion-recovery 3D turbo FLASH sequence (repetition time = 2250 ms, echo time = 3.26 ms, flip angle =  $9^\circ$ , inversion time = 900 ms) at  $1\text{ mm}^3$  isotropic spatial resolution. All functional MRI measures were based on a gradient-echo echo planar imaging sequence (repetition time = 2000 ms, echo time = 30 ms, flip angle  $70^\circ$ ) at  $3\text{ mm}^3$  isotropic spatial resolution. We acquired 33 consecutive slices in an axial-to-coronal orientation roughly parallel to the intercommissural plane, covering the whole brain ( $64 \times 64 \times 33$ ). All images were corrected for motion in k-space as supplied by the manufacturer (Siemens Healthineers). Diffusion-weighted MRI was performed using a spin-echo echo planar imaging technique at  $1.9\text{ mm}$  isotropic resolution (repetition time = 10 100 ms, echo time = 93 ms, parallel acquisition factor 2; acquisition matrix:  $128 \times 128$ , 74 sections), acquiring 64 image volumes with diffusion weighting (along 64 diffusion directions,  $b = 1000\text{ s/mm}^2$ ) and one reference image without diffusion weighting.

## TBSS analysis

All diffusion-weighted MRI images were visually inspected for artefacts, which resulted in the exclusion of diffusion-weighted

volumes (maximal four volumes) in three adults who stutter. Images were processed with tools from the FMRIB Software Library [FSL, <http://www.fmrib.ox.ac.uk/fsl/> (Jenkinson *et al.*, 2012)]. Images were corrected for eddy currents and head motion by using affine registration to the non-diffusion volumes. For each voxel the diffusion tensor was calculated, and fractional anisotropy of the tensor as well as mean diffusivity, axial diffusivity (Behrens *et al.*, 2003, 2007), and radial diffusivity were calculated. White matter skeleton-based voxel-wise statistical analysis of the fractional anisotropy data was carried out using the FSL tool TBSS (Smith *et al.*, 2006). Therefore, the fractional anisotropy images of all participants were non-linearly registered to the image of the most typical brain. All images were then averaged, and a common white matter skeleton was created. For each brain, the local maximum close to the computed skeleton was projected to the skeleton for analysis. The data for the two groups were compared at each voxel location in the skeleton using randomization statistics. Reported clusters on the skeleton were considered significant at  $P < 0.002$  at voxel level and exceeded a cluster size significance at  $P < 0.05$  based on global smoothness estimation on the skeleton, computed with AFNI (version 16.1.28, [http://ADD\\_URL](http://ADD_URL), 3dClusterSim and 3dFWHMx, (Cox, 1996). Bi-sided thresholding resulted in a cluster size threshold of  $k \geq 11$ . Subsequently, significant clusters were projected to the native space of each participant to extract further diffusion properties (mean, axial, and radial diffusivity).

## TBSS-based tractography

To reconstruct the fibre pathways that run through the significant TBSS clusters, first, a two-fibre probabilistic diffusion model was computed in every voxel using bedpostx, implemented in FSL (Behrens *et al.*, 2003, 2007). Individual TBSS clusters were used as seed masks to compute fibre pathways with FSL probtrackx (Behrens *et al.*, 2003, 2007) using the default parameters (5000 sample per voxel, curvature threshold 0.2, maximum number of steps 2000, step length 0.5 mm, loopcheck enabled). Resulting connection probability maps were scaled by calculating the logarithm of the number of computed connections in each voxel divided by the logarithm of the total number of streamlines initialized ( $5000 \times$  number of voxels). This resulted in images with normalized connection strength (connection probability distribution maps) between 0 and 1 in each voxel and allowed the following processing steps. Normalized connection maps were warped to the Montreal Neurological Institute (MNI) space and an average connectivity map was created and thresholded at 0.2 to exclude spurious connections.

## Crossing-fibre measures

The diffusion tensor-based measures such as fractional anisotropy and radial diffusivity can only explain the underlying white matter microstructure to a limited extent in regions with crossing fibres. To analyse the origin of fractional anisotropy differences in areas with two fibre populations, the probability of the major fibre direction (F1) and of the secondary fibre direction (F2) were extracted from the clusters, which showed significant differences in the TBSS analysis.

## Functional MRI

### Task

To reveal the crucial functional brain region a task was adopted from a previous publication (Riecker *et al.*, 2000) and was described in more detail in a previous study from our lab (Neef *et al.*, 2016). Three functional MRI scanning runs were carried out. Each run consisted of 12 repetitions of a speech condition and 12 repetitions of a humming condition, in a random order. During the speech condition participants imagined themselves reciting the months of the year in a continuous, fluid manner. During the humming condition participants imagined humming the non-lyrical tune of a serenade (W.A. Mozart's, *Eine kleine Nachtmusik*, KV 525). A trial was initiated by a visual cue. After 6 s, a plus symbol signalled participants to stop imagining and rest for the following 18 s. A run lasted 10 min. Two adults who stutter only finished two runs. Prior to the experiment, participants listened to the melody and performed the tasks outside the scanner to become familiarized with the test materials.

### Analysis

Functional MRI data processing was carried out with FEAT, version 6.0, a tool from the FMRIB Software library (FSL; <http://fsl.fmrib.ox.ac.uk>). Preprocessing involved motion correction, smoothing with a Gaussian kernel of 8 mm full-width at half-maximum. Non-brain tissue was removed and all volumes were intensity-normalized. Temporal high-pass filtering was achieved by Gaussian-weighted least-squares straight line fitting, with a high-pass filter cut-off at 100 s. Functional images were spatially aligned to their respective anatomical image by affine registration (Jenkinson and Smith, 2001). A further non-linear registration of the anatomical images to the standard MNI152 template brain (Andersson *et al.*, 2007) served to normalize the functional images. Boxcar models were convolved with a Gamma function. Model fit was determined by statistical time-series analysis in the framework of the general linear model. A fraction of the temporal derivative of the blurred original waveform was added to achieve a slightly better fit to the data. Across the three runs we calculated within-subject contrasts of imagining speaking > imagining melody humming and imagining melody humming > imagining speaking with a fixed-effect analysis. Across participants, mixed-effects group analyses were calculated.  $Z$  (Gaussianized T/F) statistic images were thresholded using clusters determined by  $Z > 2.3$  and a corrected cluster significance threshold of  $P < 0.05$  (Worsley *et al.*, 1996).

### Tractography

To reconstruct the fibre pathways that originate in hyperactive right frontal brain regions in adults who stutter, significant clusters from the functional MRI analysis were used as seed masks for tractography. Protrackx parameters, normalization, and alignment with standard space were kept constant. Connection probability maps were then correlated for every voxel with stuttering severity scores (SSI-4, OASES) using FSL randomise (Anderson and Robinson, 2001; Winkler *et al.*, 2014). Reported clusters in the tract volumes were significant at  $P < 0.005$  at voxel-level and exceeded a cluster size significant at  $P < 0.01$  based on global smoothness estimation

of the connectivity maps in the thresholded tractography volume with AFNI (version 16.1.28, 3dClusterSim and 3dFWHMx) (Cox, 1996). Bi-sided thresholding resulted in the following cluster size thresholds, for the tract volume of the IFG  $k \geq 169$ , for the tract volume of the frontal pole (FP)  $k \geq 145$ , and for the tract volume of the MFG  $k \geq 101$ .

## Results

### Group comparison with whole-brain TBSS

TBSS results are illustrated in Fig. 1. Compared to control participants, adults who stutter showed a reduced fractional anisotropy in the left SLF/arcuate fasciculus (MNI:  $-35, -5, 22$ ;  $k = 51$ ), in the parietal part of the right SLF II (MNI:  $30, -32, 40$ ;  $k = 40$ ), and in the right FAT (MNI:  $31, 7, 28$ ;  $k = 27$ ) close to the precentral sulcus.

### Diffusion properties and crossing fibre measures

All clusters with a reduced fractional anisotropy in adults who stutter showed an increased radial diffusivity and an increased mean diffusivity, whereas the major fibre direction (F1) was reduced in adults who stutter compared to controls (Fig. 1). This more fine-grained analysis characterizes the significant differences in the fractional anisotropy analysis, but cannot be tested statistically.

### TBSS-based tractography

With the probabilistic tractography we reconstructed fibre paths that link the significant TBSS clusters with cortical and subcortical regions (Fig. 2). Specifically, the cluster in the left SLF/arcuate fasciculus is most likely connected with the left IFG pars opercularis and pars triangularis, precentral and postcentral cortex, insula, posterior superior temporal gyrus, planum temporale, and posterior middle temporal gyrus. Subcortically, fibres run through the anterior limb of the internal capsule as well as through the external capsule, thereby reaching and passing the putamen, caudate, and thalamus towards the brainstem, where the tractogram involves fibres of the anterior thalamic radiation, cortical spinal/pontine tract, and cerebellar peduncle.

The cluster in the right SLF II is most likely connected to the right IFG pars opercularis, the MFG, precentral, postcentral, superior parietal, inferior parietal regions of the right hemisphere. Subcortically, fibres run through the posterior limb of the internal capsule as well as through the external capsule, thereby passing the putamen, caudate, and thalamus towards the brainstem where the tractogram involves fibres of the superior thalamic radiation and the cortical spinal/pontine tract.

The cluster in the right FAT is most likely connected to the right IFG pars opercularis, SMA, MFG, and precentral

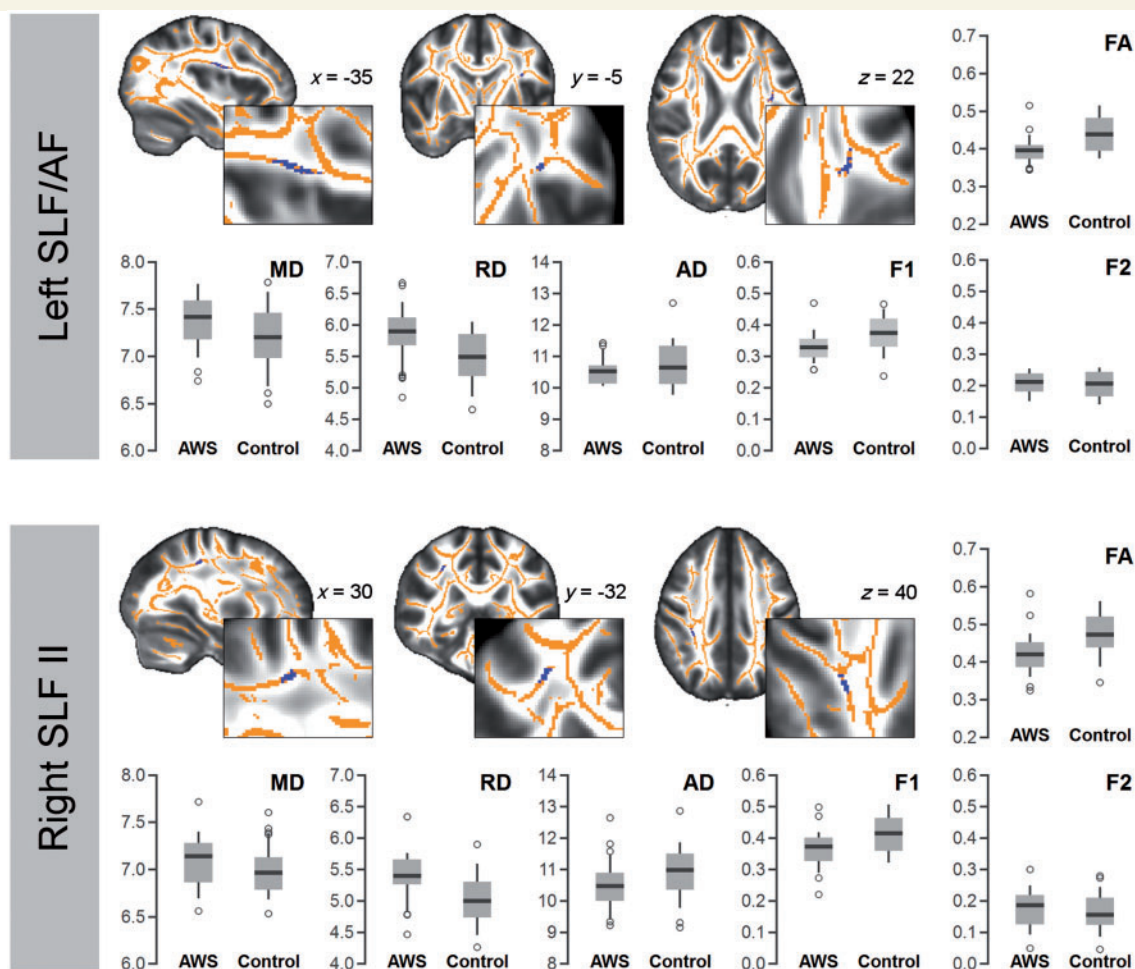


**Figure 1** Diffusion properties of the three regions with a reduced fractional anisotropy in adults who stutter, determined by whole brain TBSS. AD = axial diffusivity; AF = arcuate fasciculus; F1 = major fibre direction; F2 = secondary fibre direction; FA = fractional anisotropy; MD = mean diffusivity; RD = radial diffusivity.

gyrus. Fibre paths involve the right SLF, right anterior thalamic radiation, and transcallosal fibres through the body of the corpus callosum, which reach the superior corona radiata in the left hemisphere.

All TBSS-based tract volumes are provided as a 3D animation at: [http://openscience.cbs.mpg.de/1/tbss\\_seeds.webm](http://openscience.cbs.mpg.de/1/tbss_seeds.webm).

## Functional MRI results

Group comparisons of imagining speaking > imagining melody humming revealed an increased activation in the right frontal pole, right posterior IFG pars opercularis adjacent to the precentral gyrus, and right medial frontal gyrus (Table 2 and Fig. 3). No other differences occurred. The Supplementary material summarizes the results of imagining speaking > imagining melody humming and imagining melody humming > imagining speaking across all participants (Supplementary Tables 3 and 4) and for each group separately (Supplementary Tables 5–8).

## Functional MRI-based tractography

To show which fibre pathways originate from the hyperactive right frontal regions in adults who stutter and whether adults who stutter have altered connectivity profiles, we computed probabilistic tractography of the involved fibre tracts. Resulting tractograms are shown in the middle column in Fig. 3.

The tractogram of the cluster in the right frontal pole involves connections to the superior frontal gyrus, MFG, frontal orbital cortex, anterior insular cortex. Fibre tracts included are (i) the anterior thalamic radiation towards the medial dorsal nucleus and the anterior nucleus of the right thalamus; (ii) transcallosal fibres through the forceps minor towards contralateral homologue regions of the frontal pole; and (iii) the uncinate fasciculus towards the posterior insular cortex and the superior temporal gyrus (see also [http://openscience.cbs.mpg.de/1/seed\\_rightFP.webm](http://openscience.cbs.mpg.de/1/seed_rightFP.webm)).

The tractogram of the cluster in the right posterior IFG (pars opercularis) involves connections to the adjacent IFG

pars triangularis, precentral gyrus, and MFG. Fibre tracts included are (i) the FAT towards the preSMA and SMA; (ii) the SLF towards the anterior intraparietal sulcus; (iii) transcallosal fibres through the callosal body towards the superior corona radiata of the contralateral hemisphere; and (iv) corticospinal tract passing through the posterior limb of the internal capsule, passing the putamen, the ventral lateral nucleus of the right thalamus, subthalamic nucleus, and cerebellar peduncle. The tractography ended in the brainstem at the level of the pons (see also [http://openscience.cbs.mpg.de/1/seed\\_rightIFG.webm](http://openscience.cbs.mpg.de/1/seed_rightIFG.webm)).

The tractogram of the cluster in the right posterior MFG involves U-shaped connections to the adjacent inferior frontal sulcus, precentral gyrus, and fundus of the central sulcus. Fibre tracts included are (i) the SLF towards the superior parietal lobule; (ii) transcallosal fibres through the callosal body; and (iii) fibres through the internal capsule ending at the level of the subthalamic nucleus as suggested by the tractography (see also [http://openscience.cbs.mpg.de/1/seed\\_rightMFG.webm](http://openscience.cbs.mpg.de/1/seed_rightMFG.webm)).

## Connection probability and stuttering severity

We calculated voxel-wise correlation analyses across connection probability maps of adults who stutter ( $n = 31$ ) to

test the relationship between connection strength within each tractogram and stuttering severity as measured by the SSI-4 and the OASES. Only functional MRI-based tractograms revealed significant correlations and only with SSI-4 scores (Fig. 3). Stuttering severity was positively correlated with connection strength (i) in the right FAT when seeding in the right IFG ( $x = 25, y = 10, z = 39$ ;  $k = 246$ ); (ii) underneath the right precentral gyrus when seeding in the right MFG ( $x = 30, y = -4, z = 43$ ;  $k = 102$ ); and (iii) in the right anterior thalamic radiation when seeding in the right frontal pole ( $x = 10, y = 3, z = 7$ ;  $k = 436$ ;  $x = 26, y = 16, z = -2$ ;  $k = 121$ ). Stuttering severity was negatively correlated with connection strength in the right uncinate fasciculus/extreme capsule fibre system when seeding in the frontal pole ( $x = 31, y = 7, z = 43$ ;  $k = 327$ ).

## Discussion

In this study, we analysed white matter brain structures in adults who stutter and those who do not. The outcome of this study is 2-fold. First, we have shown that stuttering severity is linked to the strength of white matter connections of hyperactive right frontal brain regions. This brain structure–behaviour relationship incorporates affected right frontal spatially separated cortical regions into disparate networks, thereby not only pinpointing areas of pathology, but advancing circuit-based interpretations of the neuronal basis of this disorder. The second valuable achievement of this study constitutes the findings of reduced white matter integrity in the bilateral SLF and the right FAT of adults who stutter. We calculated TBSS to enable comparison with previous DTI studies. Our large sample sizes and the stringent correction for multiple comparisons validated these findings that were inconsistently reported among previous studies.

## Affected right frontal areas are not primarily linked to speech behaviour

In adults who stutter, right frontal hyperactive areas resulted from a functional MRI contrast between two motor imagery tasks, imagining speaking versus imagining humming. The three hyperactive regions, the posterior IFG, MFG, and frontal pole engage different networks and different cognitive resources, which are all relevant for

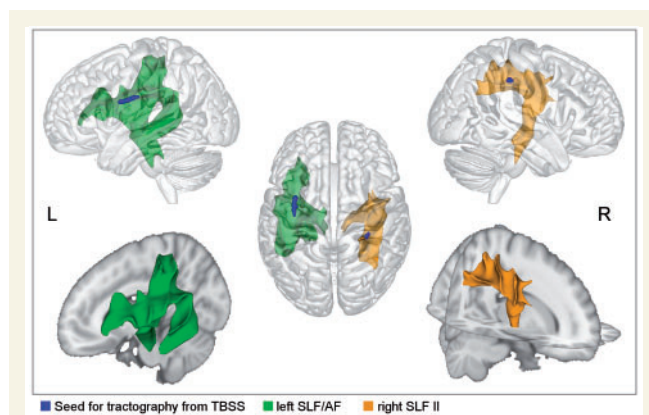


**Figure 2** TBSS-based tractography indicate involved fibre tracts. The left tract connects the IFG with postcentral, superior parietal, and superior and middle temporal regions. On the right, precentral regions are connected to postcentral and inferior parietal regions (yellow).

**Table 2** Brain activation in adults who stutter > control in speaking > humming ( $Z = 2.3, P = 0.05$ )

Brain area	MNI-coordinates			Extent (voxels)	Z-score
	x	y	z		
Right frontal pole	22	50	-2	254	3.95
Right inferior frontal gyrus (BA 44)	58	8	16	179	3.17
Right middle frontal gyrus	36	4	52	127	3.5

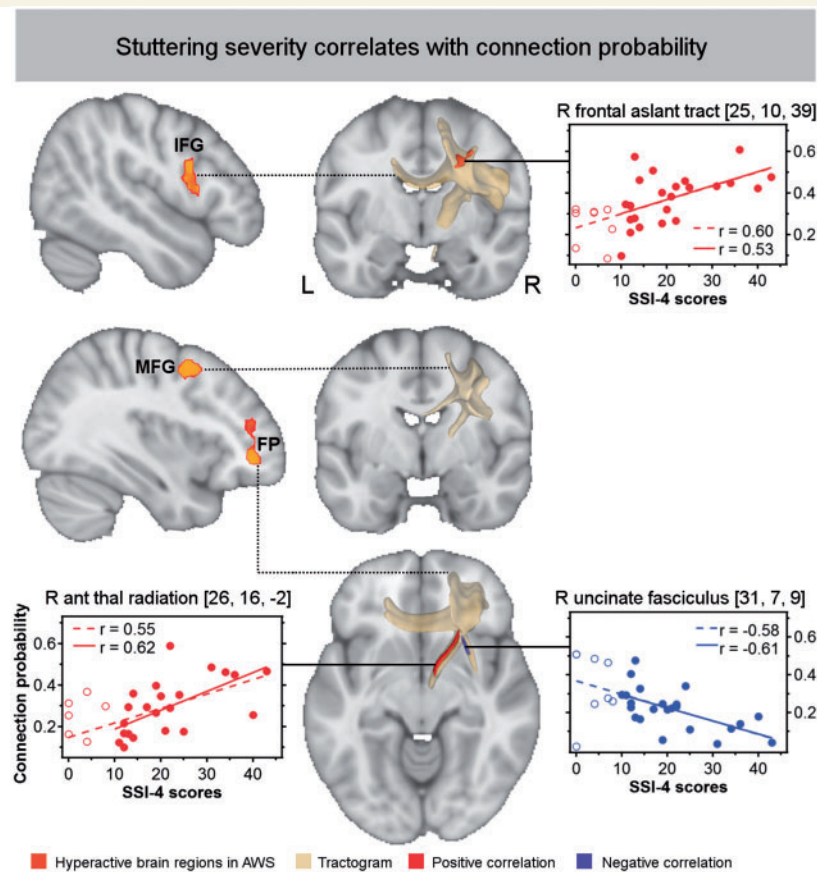


**Figure 3 Probabilistic fibre tracking seeding in right frontal regions with increased blood oxygen level-dependent activity in adults who stutter.** The connection probability was correlated with stuttering severity. Correlation coefficients are given for all adults who stutter in the upper line ( $n = 31$ , dotted line) and for those with SSI-4 > 10 in the lower line ( $n = 23$ , solid line). Positive correlations are displayed in red, negative correlation in blue, cluster-size corrected,  $P < 0.005$ ,  $\alpha < 0.01$ , two-sided.

carrying out the task. However, these areas are not primarily linked to speech behaviour.

The functional specialization in the right posterior IFG, the pars opercularis (BA 44), is manifold. Neuroimaging studies associate this region with motor imagery (Lacourse *et al.*, 2005; Guillot *et al.*, 2008), imitation and action observation (Heiser *et al.*, 2003; Molnar-Szakacs *et al.*, 2005; Kilner *et al.*, 2009), proactive and reactive working memory control (Marklund and Persson, 2012), task switching, cognitive flexibility and go/no-go control (Buchsbaum *et al.*, 2005; Hirose *et al.*, 2009). Part of the right posterior IFG implements the control of response inhibition, which comprises cognitive and motor inhibition (Aron and Poldrack, 2006; Chambers *et al.*, 2006; Li *et al.*, 2006, 2008; Aron *et al.*, 2014; Cai *et al.*, 2014b). The MFG is likewise involved in various operations that are associated with higher-level executive functions and decision-related processes (Talati and Hirsch, 2005). Similar to the right IFG, the right MFG is active during imagery tasks, stop-signal and go/no-go tasks (Rubia *et al.*, 2001; Yoo *et al.*, 2001; Zheng *et al.*, 2008; Sebastian *et al.*, 2013). Given a large body of literature that associates

these two cortical regions with aspects of imagery and inhibition, it is intriguing that an overactivation of these structures is a neural sign of stuttering.

The functional MRI task in the current study involved reactive inhibition because participants were asked to stop the speech motor imagery. In our previous study we conducted an independent component analysis thereby showing that the activation of the right posterior IFG, the pars opercularis, was related to both aspects of the task. Speech motor imagery is necessary to realize the task and reactive inhibition to stop this realization (Neef *et al.*, 2016). Taking this line of thinking one step further, the imaginary task itself involves continuous inhibitory control in order to prevent overt motor responses. Accordingly, the involvement of the right IFG, the pars opercularis, during imagining speaking might be primarily associated with an executive control over action, concretely, the suppression of overt speech. This view would be consistent with the observation that imagining speaking recruits the right IFG (Tian *et al.*, 2016), whereas overt speaking does not involve the right posterior IFG but the left hemisphere homologue (Turkeltaub *et al.*, 2002; Ghosh *et al.*, 2008; Guenther,

2016). It is tempting to speculate that the stronger recruitment of the right posterior IFG in stuttering is related to imagery and inhibitory control mechanisms rather than to processes that support compensation. And indeed, a recent behavioural study supports the idea that the motor control deficit in stuttering involves impaired motor inhibition (Markett *et al.*, 2016). Thus, behavioural and neuroimaging studies accumulate evidence for an affected response inhibition mechanism in stuttering.

The third region that showed hyperactivity in adults who stutter was the right frontal pole. The function of the right frontal pole is poorly understood. Its involvement could be related to domain-general functions, such as task monitoring (Koechlin and Hyafil, 2007) or attentional gating (Burgess *et al.*, 2007). The observation of an amplified involvement of regions that support imagery and attentional allocation to the self-generated representations suggests that speaking imagery was more challenging for a system that repeatedly fails to produce fluent speech. This view would be compatible with possible compensation mechanisms. An alternative view would be that these hyperactivations reflect an activation pattern inherent to the disorder and thus would signal maladaptive or causal activity even in the state of covert speech behaviour.

In summary, it is intriguing that none of the right frontal hyperactive regions is primarily involved in speech production in fluent speakers (Turkeltaub *et al.*, 2002; Ghosh *et al.*, 2008; Guenther, 2016). Rather, right IFG and MFG are involved in the ability to apply executive control over actions, while the frontal pole contributes to the ability to stay focused on a given task.

## Severity of stuttering is related to increased structural connectivity of the motor response inhibition network

Right posterior IFG and MFG, however, are not solely responsible for response inhibition. Rather, they are part of large-scale networks that also include the right SMG, preSMA, subthalamic nucleus, and putamen. These cortical and subcortical structures are known to function together during the processing of go/no-go and stop signal tasks (Aron and Poldrack, 2006; Cai *et al.*, 2014c). This observed pattern of functional connectivity is in agreement with anatomical tracer analyses of corticocortical connections in non-human primates (Schmahmann and Pandya, 2009) and diffusion-weighted imaging studies in humans (Aron *et al.*, 2007; Neubert *et al.*, 2010). Putamen and subthalamic nucleus receive input from various brain sites and thus constitute a part of the cortico-thalamocortical loops that are regulated by cortex, basal ganglia, and cerebellum (Alexander *et al.*, 1986; Alexander and Crutcher, 1990). The tract volume of the right posterior IFG tractography reflects this connectivity at a macroanatomical scale, and hence, proves the network aspect. Moreover,

the tract volume contains key nodes of the response inhibition network, suggesting that it includes white matter structures involved in this function.

The implication of these white matter structures in the context of stuttering has already been suggested (Aron *et al.*, 2007). And indeed, our correlation analysis indicated a positive correlation between stuttering severity and the connection strength within the IFG tract volume. Our data related more severe motor signs of stuttering to stronger anatomical connections of the FAT linking the posterior IFG with SMA and preSMA. This finding indicates that the right FAT plays a crucial role in the motor aspect of the disorder, which might reflect cause or maladaptation.

The functional role of the right IFG versus the right preSMA in inhibitory control is not entirely clear yet (Aron *et al.*, 2014). However, both structures function together with the subthalamic nucleus in a network that mediates fast global inhibition. The characteristic motor signs of stuttering are silent speech blocks, sound prolongations, and sound and syllable repetitions. Common to all these symptoms is the unsuccessful control of stop and go. While speaking, the control of these processes happens rather automatically. Accordingly, an overly active global response suppression mechanism that induces an unspecific broad inhibition is a most likely pathomechanism because it would hinder the smooth successive execution of appropriate motor actions. The stronger connectivity of the right FAT might be a neuroanatomical correlate of such an overly implicated global response suppression mechanism.

## Severity of stuttering is related to increased connection strength between right frontal pole and anterior thalamic nuclei

The dorsolateral prefrontal cortex is part of the circuits constituting the non-motor basal ganglia prefrontal loop. Within these circuits, the frontal pole (BA 10) interacts with anterior thalamic nuclei (Alexander *et al.*, 1986). These circuits might regulate the initiation and termination of cognitive processes such as planning, working memory, and attention (Graybiel, 1997). While the right IFG might function together with the preSMA, subthalamic nucleus and basal ganglia circuit to regulate reactive inhibition, the right dorsolateral prefrontal cortex might function together with the caudate and the thalamus to regulate proactive inhibition (Jahanshahi *et al.*, 2015). Proactive inhibition is prospective and assumed to regulate thoughts, impulses, emotion, mood, and behaviour. In the context of stuttering this network might be implicated in response to the anticipation of stuttering. An overwhelming majority of adults who stutter often experience anticipation of stuttering (Jackson *et al.*, 2015). There are two types of reactions, avoidance strategies such as word substitution and circumlocuting, adding meaningless speech, making non-speech movement, and stalling, and self-management strategies

such as pause, change of speech rate, use of fluency-shaping or stutter-modification. Avoidance behaviour as well as self-management strategies very likely implicate circuits that regulate proactive inhibition. Until today, no neuro-imaging study on stuttering scrutinized neuronal correlates of stuttering anticipation and respective behaviour. We are the first to bring such a brain–behaviour relationship into awareness. Future studies are necessary to test this hypothesis.

### In stuttering, right frontal structural connectivity might support compensatory mechanisms

When seeding in the frontal pole, the probabilistic fibre tracking suggests connections of this region with further higher-order prefrontal areas and thalamo-cortical networks, but no connections with the primary motor or sensory cortex. Instead, reconstructed fibre pathways through the extreme capsule linked the frontal pole to higher-order auditory and multisensory areas of the superior temporal gyrus via the uncinate fasciculus. The negative correlation between stuttering severity and connection strength within the right uncinate fasciculus, suggests a compensatory role of this structure. The correlation was only evident when considering the motor aspects of stuttering (SSI-4), but not when considering emotional and social-cognitive aspects (OASES). Therefore, we can exclude that the brain structure–function relationship observed here results from the psychological strain the disorder entails. Rather, the observed correlation underscores a close link between the severity level of the motor aspect of the disorder and the right-hemispheric fronto-temporal connection strength of the ventrally located uncinate fasciculus. This finding is consistent with a previous diffusion-weighted MRI study with children who stutter; fractional anisotropy in the right uncinate fasciculus correlated negatively with stuttering severity as measured by the SSI (Chang *et al.*, 2015). The fact that children who stutter are already displaying such a brain–behaviour relationship, suggests that implicated networks support fluent speech very early on.

The view of a compensatory role of this connection finds support in a previous interpretation (Neef *et al.*, 2015) of recent functional MRI activation likelihood estimate (ALE)-meta analysis (Budde *et al.*, 2014; Belyk *et al.*, 2015), which, however, needs to be considered with caution because previous ALE meta-analyses are based on a liberal statistical thresholds and thus might involve false positive results (Belyk *et al.*, 2017; Eickhoff *et al.*, 2017). Nevertheless, when comparing functional MRI contrasts of dysfluent state and fluent state within affected individuals, it becomes evident that an additional recruitment of right superior temporal regions supports the fluent state. Presupposed, enhanced fluency requires additional cognitive efforts, such as the allocation of attention to the task and the multisensory monitoring of speech motor acts, in which

a compensatory role of the uncinate fasciculus and the solid link between right fronto-temporal regions becomes highly plausible.

### In stuttering, left and right dorsal pathways show signs of disconnection

A further important outcome of the present study is the consolidation of white matter differences in fibre pathways that are suspected of alterations in persistent stuttering. TBSS located a reduction of fractional anisotropy bilaterally in the SLF, a massive intrahemispheric fibre system that connects postrolandic regions with the frontal lobe (Catani *et al.*, 2005; Makris *et al.*, 2005). Previous TBSS studies on persistent stuttering have reported white matter differences throughout the brain (Chang *et al.*, 2008, 2015; Watkins *et al.*, 2008; Kell *et al.*, 2009; Cykowski *et al.*, 2010; Cai *et al.*, 2014a; Connally *et al.*, 2014; Civier *et al.*, 2015). Our recent meta-analysis, however, assigned most robust reductions of fractional anisotropy to the left SLF/arcuate fasciculus (Neef *et al.*, 2015), which is consistent with current observations. Effects in the left SLF are also reported in another study based the TBSS analyses with a comparably large population (Connally *et al.*, 2014). According to this study a cluster in the left SLF had an extent of 27 voxels at ( $x = -37$ ,  $y = -25$ ,  $z = 30$ ), which is close to the centre of gravity in the left SLF/arcuate fasciculus reported here. Our meta-analysis yielded no consistent cluster in the right hemisphere. Findings considering TBSS clusters of reduced fractional anisotropy in the right SLF are indeed less straight forward. A few TBSS studies report fractional anisotropy reductions along the right SLF but in different fractions (Cai *et al.*, 2014a; Chang *et al.*, 2015) when compared to the clusters found here.

Considering functions of bilateral SLF, it is important to separate two dorsal streams. It has been postulated that dorsal fibre tracts linking left BA44 and left posterior temporal cortex subserve syntactic processing (Catani *et al.*, 2005; Friederici *et al.*, 2006; Anwander *et al.*, 2007), while a different segment of the SLF (SLF III) that connects left BA 44 and BA 6 with the left supramarginal gyrus supports articulation and repetition (Makris *et al.*, 2005; Gierhan, 2013). A speech production model maps the processing of feedback control to fronto-parietal and fronto-temporal networks (Guenther *et al.*, 1998; Bohland *et al.*, 2009). Strikingly, left hemisphere feedback control is postulated to play a particular role during language acquisition; mapping sound to articulation is a crucial aspect in this period (Guenther, 1995; Perani *et al.*, 2011). In contrast, online control of perturbed auditory feedback or perturbed somatosensory feedback during speaking is primarily mediated by right hemisphere fronto-parieto-temporal networks (Tourville *et al.*, 2008; Golfopoulos *et al.*, 2011). Accordingly, our findings of bilateral white matter disorganization within dorsal fibre tracts in adults who

persist to stutter, suggest a potential importance of feedback mechanisms in this disorder throughout life span.

Complementarily, in adults who stutter, previous fibre tracking studies report a reduced fractional anisotropy in the right anterior segment of the arcuate fasciculus (Kronfeld-Duenias *et al.*, 2016b), reduced mean fractional anisotropy across the whole tract volume (Connally *et al.*, 2014), and an anomalous white matter morphology of the right posterior segment of the right arcuate fasciculus (Cieslak *et al.*, 2015). Here, fractional anisotropy was reduced in the SLF II and in the anterior segment of the SLF, a region that also contains fibres of the FAT, previously reported to be associated with stuttering (Kemerdere *et al.*, 2016; Kronfeld-Duenias *et al.*, 2016a). Thus, previous and current observations strengthen the view of a compromised intrahemispheric transfer of neural signals in stuttering that link the posterior IFG and the premotor cortex to parietal and temporal regions.

Probability maps help to assign labels to affected structures (Mori *et al.*, 2005; Wakana *et al.*, 2007; Hua *et al.*, 2008), making it possible to draw inferences about disconnected brain regions. Here, we used TBSS-based fibre tracking additionally (Fig. 2) to pinpoint affected fibre tracts. Tractograms from both hemispheres involve parts of the SLF that connect the IFG with parietal areas. Furthermore, resulting tractograms indicate possible involvement of ascending thalamo-cortical projection fibres, and descending projections to the pons, cerebellar penduncle, and the corticospinal tract, common structures of suspect (Watkins *et al.*, 2008; Connally *et al.*, 2014), as they belong to the speech-production networks implicated in stuttering (Guenther, 2016).

Two other TBSS clusters of a recent ALE meta-analysis (Neef *et al.*, 2015) have not been found in the current dataset, a cluster in the left inferior parietal lobule adjacent to the angular gyrus and the posterior division of the supra-marginal gyrus, and a cluster in the posterior midbody of the corpus callosum. This recent meta-analysis was based on seven existing DTI studies that reported foci of reduced fractional anisotropy in participants older than 14 years. Overall, the pooled set considered 60 reported foci from 121 adults who stutter and 126 fluent speakers. The quantitative GingerALE analysis (Eickhoff *et al.*, 2009) estimates the spatial uncertainty associated with each reported coordinate, thereby identifying regions which show a consistent reduction of fractional anisotropy across studies. This approach is one way of overcoming the problem of small sample sizes and low reliability inherent to previous DTI studies. Critically, seven studies have insufficient statistical power and only a few of the previous studies reported TBSS findings that were corrected for multiple comparisons. Hence, TBSS studies in the field of stuttering are susceptible to false positive findings. The advantage of the current study is that the high sample size and the applied cluster thresholding reduce this susceptibility.

The interpretation of an altered fractional anisotropy is complicated. This is particularly important in white matter

regions that contain fibre crossings and fanning. In particular, fibre crossings should be considered when interpreting current TBSS findings. For the cluster in the right FAT, for example, we cannot exclude an influence of crossing fibres of the SLF. Thus, it is unclear whether fractional anisotropy reductions result, for example, from demyelination, reduced axonal packing, or increased diameter of axon calibres of the FAT tract itself, or from a complex geometry of involved fibres. One way of disentangling this complexity is to consider further diffusion properties such as mean, radial, and axial diffusivity, and to separate the major and second major direction of streamlines passing through certain voxels (F1 and F2). Strikingly, along with a reduced fractional anisotropy, adults who stutter showed an increased radial diffusivity, an increased mean diffusivity together with a reduced F1, and no differences for F2 when compared with controls. This combination of diffusion properties was evident across all three TBSS clusters, the cluster in the left arcuate fasciculus/SLF, in the right SLF, and in the right FAT. Thus, adults who stutter seem to exhibit a weakened connectivity of fibre tracts along the major diffusion direction, which favours the view that atypical structures are insufficiently myelinated or that the axonal packing is reduced therein. It is unlikely that crossing fibres of the secondary fibre direction exhibit a stronger integrity, because in such a case F2 would be increased. Consequently, our data reinforce previous findings of a white matter deficit of the left and right SLF and the right FAT. For the additional diffusion properties, group differences were not accessed statistically to avoid circularity.

## Conclusion

Previous neuroimaging studies on persistent developmental stuttering related the hyperactivity of right frontal areas to compensatory or causal mechanisms of the disorder. This view was based on the idea that involved hyperactive regions are homologue areas of the left frontal network involved in speech production (Turkeltaub *et al.*, 2002; Ghosh *et al.*, 2008), and that its recruitment relates to interhemispheric interactions that might cause or compensate for a left hemisphere structural and functional deficit (Neumann *et al.*, 2005; Watkins *et al.*, 2008; Kell *et al.*, 2009; Chang *et al.*, 2011; Lu *et al.*, 2012; Beal *et al.*, 2015). The current study works out some details of these opposing views, thereby considering the special role of right hemisphere frontal regions in response inhibition and task monitoring. Here, we show that an increased right hemisphere structural connectivity between the posterior IFG pars opercularis, pre-SMA, and subthalamic nucleus was evident in participants with more severe stuttering, which might reflect an amplified activity of the hyperactive pathway that controls global response suppression and the ability to stop an ongoing motor response. In contrast, an increased structural connectivity of right fronto-temporal

regions supports fluency possibly by a strengthened ability to allocate attention to the multisensory monitoring of speech motor responses. Accordingly, our combined functional MRI-DTI analysis presents a new view on pathophysiological principals of stuttering and focuses on networks that specifically engage the right hemisphere.

## Acknowledgements

We are thankful to Kristina Anders for the analysis of the speech samples, Harald Euler for the provision of the German Version of the OASES, Peter Dechent for his recommendations regarding the MR sequences, and Ilona Pfahlert and Britta Perl for their help in MRI data recording.

## Funding

This work was funded by the Dorothea Schlözer Fellowship Programme of the University of Göttingen (to N.E.N.), and by the Deutsche Forschungsgemeinschaft (NE 1841/1-1 to N.E.N; and SO 429/4-1 to M.S.).

## Supplementary material

Supplementary material is available at *Brain* online.

## References

Alexander GE, Crutcher MD. Functional architecture of basal ganglia circuits: neural substrates of parallel processing. *Trends Neurosci* 1990; 13: 266–71.

Alexander GE, DeLong MR, Strick PL. parallel organization of functionally segregated circuits linking basal ganglia and cortex. *Annu Rev Neurosci* 1986; 9: 357–81.

Anderson MJ, Robinson J. Permutation tests for linear models. *Aust N Z J Stat* 2001; 43: 75–88.

Andersson JLR, Jenkinson M, Smith S. TR07JA2: Non-linear registration, aka spatial normalisation. FMRIB Analysis Group Technical Reports. 2007. Available from: <http://www.fmrib.ox.ac.uk/analysis/techrep/tr07ja2/tr07ja2.pdf>.

Anwander A, Tittgemeyer M, von Cramon D, Friederici AD, Knösche TR. Connectivity-based parcellation of Broca's area. *Cereb Cortex* 2007; 17: 816–25.

Aron AR. From reactive to proactive and selective control: developing a richer model for stopping inappropriate responses. *Biol Psychiatry* 2011; 69: e55–68.

Aron AR, Behrens TE, Smith S, Frank MJ, Poldrack RA. Triangulating a cognitive control network using diffusion-weighted magnetic resonance imaging (MRI) and functional MRI. *J Neurosci* 2007; 27: 3743–52.

Aron AR, Poldrack RA. Cortical and subcortical contributions to stop signal response inhibition: role of the subthalamic nucleus. *J Neurosci* 2006; 26: 2424–33.

Aron AR, Robbins TW, Poldrack RA. Inhibition and the right inferior frontal cortex: one decade on. *Trends Cogn Sci* 2014; 18: 177–85.

Beal DS, Lerch JP, Cameron B, Henderson R, Gracco VL, De Nil LF. The trajectory of gray matter development in Broca's area is abnormal in people who stutter. *Front Hum Neurosci* 2015; 9: 89.

Behrens TEJ, Berg HJ, Jbabdi S, Rushworth MFS, Woolrich MW. Probabilistic diffusion tractography with multiple fibre orientations: what can we gain? *Neuroimage* 2007; 34: 144–55.

Behrens TEJ, Woolrich MW, Jenkinson M, Johansen-Berg H, Nunes RG, Clare S, et al. Characterization and propagation of uncertainty in diffusion-weighted MR imaging. *Magn Reson Med* 2003; 50: 1077–88.

Belyk M, Kraft SJ, Brown S. Stuttering as a trait or state—an ALE meta-analysis of neuroimaging studies. *Eur J Neurosci* 2015; 41: 275–84.

Belyk M, Kraft SJ, Brown S. Stuttering as a trait or a state revisited: motor system involvement in persistent developmental stuttering. *Eur J Neurosci* 2017; 45: 622–4.

Bloodstein O, Ratner NB. A Handbook on stuttering. Clifton Park, NY: Delmar Learning; 2008.

Bohland JW, Bullock D, Guenther FH. Neural representations and mechanisms for the performance of simple speech sequences. *J Cogn Neurosci* 2009; 22: 1504–29.

Buchsbaum BR, Greer S, Chang W-L, Berman KF. Meta-analysis of neuroimaging studies of the Wisconsin Card-Sorting task and component processes. *Hum Brain Mapp* 2005; 25: 35–45.

Budde KS, Barron DS, Fox PT. Stuttering, induced fluency, and natural fluency: a hierarchical series of activation likelihood estimation meta-analyses. *Brain Lang* 2014; 139: 99–107.

Burgess PW, Dumontheil I, Gilbert SJ. The gateway hypothesis of rostral prefrontal cortex (area 10) function. *Trends Cogn Sci* 2007; 11: 290–8.

Bütfering C. Geschlechtsspezifische Unterschiede sprechassoziierter Gehirnakktivität bei stotternden. Menschen: Eine klinische Studie mittels funktioneller Magnetresonanztomographie; 2015.

Cai S, Tourville JA, Beal DS, Perkell JS, Guenther FH, Ghosh SS. Diffusion imaging of cerebral white matter in persons who stutter: evidence for network-level anomalies. *Front Hum Neurosci* 2014a; 8: 54.

Cai W, Cannistraci CJ, Gore JC, Leung H-C. Sensorimotor-independent prefrontal activity during response inhibition. *Hum Brain Mapp* 2014b; 35: 2119–36.

Cai W, Ryali S, Chen T, Li C-SR, Menon V. Dissociable roles of right inferior frontal cortex and anterior insula in inhibitory control: evidence from intrinsic and task-related functional parcellation, connectivity, and response profile analyses across multiple datasets. *J Neurosci* 2014c; 34: 14652–67.

Catani M, Dell'Acqua F, Vergani F, Malik F, Hodge H, Roy P, et al. Short frontal lobe connections of the human brain. *Cortex* 2012; 48: 273–91.

Catani M, Jones DK, Ffytche DH. Perisylvian language networks of the human brain. *Ann Neurol* 2005; 57: 8–16.

Chambers CD, Bellgrove MA, Stokes MG, Henderson TR, Garavan H, Robertson IH, et al. Executive 'brake failure' following deactivation of human frontal lobe. *J Cogn Neurosci* 2006; 18: 444–55.

Chang SE, Erickson KI, Ambrose NG, Hasegawa-Johnson MA, Ludlow CL. Brain anatomy differences in childhood stuttering. *Neuroimage* 2008; 39: 1333.

Chang SE, Horwitz B, Ostuni J, Reynolds R, Ludlow CL. Evidence of left inferior frontal–premotor structural and functional connectivity deficits in adults who stutter. *Cereb Cortex* 2011; 21: 2507–18.

Chang SE, Kenney MK, Loucks TMJ, Ludlow CL. Brain activation abnormalities during speech and non-speech in stuttering speakers. *Neuroimage* 2009; 46: 201–12.

Chang SE, Zhu DC, Choo AL, Angstadt M. White matter neuroanatomical differences in young children who stutter. *Brain* 2015; 138: 694–711.

Chesters J, Watkins KE, Möttönen R. Investigating the feasibility of using transcranial direct current stimulation to enhance fluency in people who stutter. *Brain Lang* 2017; 164: 68–76.

Cieslak M, Ingham RJ, Ingham JC, Grafton ST. Anomalous white matter morphology in adults who stutter. *J Speech Lang Hear Res* 2015; 58: 268–77.

- Civier O, Kronfeld-Duenias V, Amir O, Ezrati-Vinacour R, Ben-Shachar M. Reduced fractional anisotropy in the anterior corpus callosum is associated with reduced speech fluency in persistent developmental stuttering. *Brain Lang* 2015; 143: 20–31.
- Connally EL, Ward D, Howell P, Watkins KE. Disrupted white matter in language and motor tracts in developmental stuttering. *Brain Lang* 2014; 131: 25–35.
- Cox RW. AFNI: software for analysis and visualization of functional magnetic resonance neuroimages. *Comput Biomed Res Int J* 1996; 29: 162–73.
- Craig-McQuaide A, Akram H, Zrinzo L, Tripoliti E. A review of brain circuitries involved in stuttering. *Front Hum Neurosci* 2014; 8: 884.
- Cykowski MD, Fox PT, Ingham RJ, Ingham JC, Robin DA. A study of the reproducibility and etiology of diffusion anisotropy differences in developmental stuttering: a potential role for impaired myelination. *Neuroimage* 2010; 52: 1495–504.
- De Nil LF, Kroll RM, Kapur S, Houle S. A positron emission tomography study of silent and oral single word reading in stuttering and nonstuttering adults. *J Speech Lang Hear Res* 2000; 43: 1038–53.
- Eickhoff SB, Laird AR, Fox PM, Lancaster JL, Fox PT. Implementation errors in the GingerALE software: description and recommendations. *Hum Brain Mapp* 2017; 38: 7–11.
- Eickhoff SB, Laird AR, Grefkes C, Wang LE, Zilles K, Fox PT. Coordinate-based activation likelihood estimation meta-analysis of neuroimaging data: a random-effects approach based on empirical estimates of spatial uncertainty. *Hum Brain Mapp* 2009; 30: 2907–26.
- Etchell AC, Johnson BW, Sowman PF. Behavioral and multimodal neuroimaging evidence for a deficit in brain timing networks in stuttering: a hypothesis and theory. *Front Hum Neurosci* 2014; 8: 467.
- Fox PT, Ingham RJ, Ingham JC, Hirsch TB, Downs JH, Martin C, et al. A PET study of the neural systems of stuttering. *Nature* 1996; 382: 158–62.
- Fox PT, Ingham RJ, Ingham JC, Zamarripa F, Xiong J-H, Lancaster JL. Brain correlates of stuttering and syllable production: A PET performance-correlation analysis. *Brain* 2000; 123: 1985–2004.
- Friederici AD, Bahlmann J, Heim S, Schubotz RI, Anwander A. The brain differentiates human and non-human grammars: Functional localization and structural connectivity. *Proc Natl Acad Sci USA* 2006; 103: 2458–63.
- Ghosh SS, Tourville JA, Guenther FH. A neuroimaging study of pre-motor lateralization and cerebellar involvement in the production of phonemes and syllables. *J Speech Lang Hear Res* 2008; 51: 1183–202.
- Gierhan SME. Connections for auditory language in the human brain. *Brain Lang* 2013; 127: 205–21.
- Golfinopoulos E, Tourville JA, Bohland JW, Ghosh SS, Nieto-Castanon A, Guenther FH. fMRI investigation of unexpected somatosensory feedback perturbation during speech. *Neuroimage* 2011; 55: 1324–38.
- Graybiel AM. The basal ganglia and cognitive pattern generators. *Schizophr Bull* 1997; 23: 459–69.
- Guenther FH. Speech sound acquisition, coarticulation, and rate effects in a neural network model of speech production. *Psychol Rev* 1995; 102: 594–21.
- Guenther FH. Neural control of speech [Internet]. Cambridge, MA: MIT Press; 2016. Available from: <https://mitpress.mit.edu/books/neural-control-speech> (9 September 2016, date last accessed).
- Guenther FH, Hampson M, Johnson D. A theoretical investigation of reference frames for the planning of speech movements. *Psychol Rev* 1998; 105: 611–33.
- Guillot A, Collet C, Nguyen VA, Malouin F, Richards C, Doyon J. Functional neuroanatomical networks associated with expertise in motor imagery. *Neuroimage* 2008; 41: 1471–83.
- Heiser M, Iacoboni M, Maeda F, Marcus J, Mazziotta JC. The essential role of Broca's area in imitation. *Eur J Neurosci* 2003; 17: 1123–8.
- Hickok G, Poeppel D. The cortical organization of speech processing. *Nat Rev Neurosci* 2007; 8: 393–402.
- Hirose S, Chikazoe J, Jimura K, Yamashita K, Miyashita Y, Konishi S. Sub-centimeter scale functional organization in human inferior frontal gyrus. *Neuroimage* 2009; 47: 442–50.
- Hua K, Zhang J, Wakana S, Jiang H, Li X, Reich DS, et al. Tract probability maps in stereotaxic spaces: analyses of white matter anatomy and tract-specific quantification. *Neuroimage* 2008; 39: 336–47.
- Ingham RJ, Grafton ST, Bothe AK, Ingham JC. Brain activity in adults who stutter: Similarities across speaking tasks and correlations with stuttering frequency and speaking rate. *Brain Lang* 2012; 122: 11–24.
- Iverach L, Rapee RM. Social anxiety disorder and stuttering: current status and future directions. *J Fluency Disord* 2014; 40: 69–82.
- Jackson ES, Yaruss JS, Quesal RW, Terranova V, Whalen DH. Responses of adults who stutter to the anticipation of stuttering. *J Fluency Disord* 2015; 45: 38–51.
- Jahanshahi M, Obeso I, Rothwell JC, Obeso JA. A fronto-striato-subthalamic-pallidal network for goal-directed and habitual inhibition. *Nat Rev Neurosci* 2015; 16: 719–32.
- Jenkinson M, Beckmann CF, Behrens TEJ, Woolrich MW, Smith SM. FSL. *Neuroimage* 2012; 62: 782–90.
- Jenkinson M, Smith S. A global optimisation method for robust affine registration of brain images. *Med Image Anal* 2001; 5: 143–56.
- Kell CA, Neumann K, von Kriegstein K, Posenenske C, von Gudenberg AW, Euler H, et al. How the brain repairs stuttering. *Brain* 2009; 132: 2747–60.
- Kemerdere R, de Champfleury NM, Deverdun J, Cochereau J, Moritz-Gasser S, Herbet G, et al. Role of the left frontal aslant tract in stuttering: a brain stimulation and tractographic study. *J Neurol* 2016; 263: 157–67.
- Kilner JM, Neal A, Weiskopf N, Friston KJ, Frith CD. Evidence of mirror neurons in human inferior frontal gyrus. *J Neurosci* 2009; 29: 10153–9.
- Koechlin E, Hyafil A. Anterior prefrontal function and the limits of human decision-making. *Science* 2007; 318: 594–8.
- Koedoot C, Bouwmans C, Franken M-C, Stolk E. Quality of life in adults who stutter. *J Commun Disord* 2011; 44: 429–43.
- Kronfeld-Duenias V, Amir O, Ezrati-Vinacour R, Civier O, Ben-Shachar M. The frontal aslant tract underlies speech fluency in persistent developmental stuttering. *Brain Struct Funct* 2016; 221: 365–81.
- Kronfeld-Duenias V, Amir O, Ezrati-Vinacour R, Civier O, Ben-Shachar M. Dorsal and ventral language pathways in persistent developmental stuttering. *Cortex* 2016b; 81: 79–92.
- Lacourse MG, Orr ELR, Cramer SC, Cohen MJ. Brain activation during execution and motor imagery of novel and skilled sequential hand movements. *Neuroimage* 2005; 27: 505–19.
- Li CR, Huang C, Constable RT, Sinha R. Imaging response inhibition in a stop-signal task: neural correlates independent of signal monitoring and post-response processing. *J Neurosci* 2006; 26: 186–92.
- Li C-SR, Yan P, Sinha R, Lee T-W. Subcortical processes of motor response inhibition during a stop signal task. *Neuroimage* 2008; 41: 1352–63.
- Lu C, Chen C, Ning N, Ding G, Guo T, Peng D, et al. The neural substrates for atypical planning and execution of word production in stuttering. *Exp Neurol* 2010; 221: 146–56.
- Lu C, Chen C, Peng D, You W, Zhang X, Ding G, et al. Neural anomaly and reorganization in speakers who stutter: a short-term intervention study. *Neurology* 2012; 79: 625–32.
- Makris N, Kennedy DN, McInerney S, Sorensen AG, Wang R, Caviness VS, et al. Segmentation of subcomponents within the superior longitudinal fascicle in humans: a quantitative, *in vivo*, DT-MRI study. *Cereb Cortex* 2005; 15: 854–69.
- Markett S, Bleek B, Reuter M, Prüss H, Richardt K, Müller T, et al. Impaired motor inhibition in adults who stutter—evidence from

- speech-free stop-signal reaction time tasks. *Neuropsychologia* 2016; 91: 444–50.
- Marklund P, Persson J. Context-dependent switching between proactive and reactive working memory control mechanisms in the right inferior frontal gyrus. *Neuroimage* 2012; 63: 1552–60.
- Molnar-Szakacs I, Iacoboni M, Koski L, Mazziotta JC. Functional segregation within pars opercularis of the inferior frontal gyrus: evidence from fMRI studies of imitation and action observation. *Cereb Cortex* 2005; 15: 986–94.
- Mori S, Wakana S, Zijl PCM van, Nagae-Poetscher LM. MRI atlas of human white matter. Amsterdam: Elsevier; 2005.
- Morris DM, Embleton KV, Parker GJM. Probabilistic fibre tracking: differentiation of connections from chance events. *Neuroimage* 2008; 42: 1329–39.
- Nambu A, Tokuno H, Takada M. Functional significance of the cortico-subthalamic-pallidal ‘hyperdirect’ pathway. *Neurosci Res* 2002; 43: 111–17.
- Neef NE, Anwender A, Friederici AD. The neurobiological grounding of persistent stuttering: from structure to function. *Curr Neurol Neurosci Rep* 2015; 15: 1–11.
- Neef NE, Jung K, Rothkegel H, Pollok B, von Gudenberg AW, Paulus W, et al. Right-shift for non-speech motor processing in adults who stutter. *Cortex* 2011; 47: 945–54.
- Neef NE, Bütfering C, Anwender A, Friederici AD, Paulus W, Sommer M. Left posterior-dorsal area 44 couples with parietal areas to promote speech fluency, while right area 44 activity promotes the stopping of motor responses. *Neuroimage* 2016; 142: 628–44.
- Neubert F-X, Mars RB, Buch ER, Olivier E, Rushworth MFS. Cortical and subcortical interactions during action reprogramming and their related white matter pathways. *Proc Natl Acad Sci USA* 2010; 107: 13240–5.
- Neumann K, Euler HA, von Gudenberg AW, Giraud A-L, Lanfermann H, Gall V, et al. The nature and treatment of stuttering as revealed by fMRI: a within- and between-group comparison. *J Fluency Disord* 2003; 28: 381–410.
- Neumann K, Preibisch C, Euler HA, von Gudenberg AW, Lanfermann H, Gall V, et al. Cortical plasticity associated with stuttering therapy. *J Fluency Disord* 2005; 30: 23–39.
- Oldfield RC. The assessment and analysis of handedness: the Edinburgh inventory. *Neuropsychologia* 1971; 9: 97–113.
- Perani D, Saccuman MC, Scifo P, Anwender A, Spada D, Baldoli C, et al. Neural language networks at birth. *Proc Natl Acad Sci USA* 2011; 108: 16056–61.
- Preibisch C, Neumann K, Raab P, Euler HA, von Gudenberg AW, Lanfermann H, et al. Evidence for compensation for stuttering by the right frontal operculum. *Neuroimage* 2003; 20: 1356–64.
- Riecker A, Ackermann H, Wildgruber D, Dogil G, Grodd W. Opposite hemispheric lateralization effects during speaking and singing at motor cortex, insula and cerebellum. [Miscellaneous Article]. *Neuroreport* 2000; 11: 1997–2000.
- Riley GD. Stuttering severity instrument, Fourth Edition (SSI-4). 4th edn. Austin: Pro-Ed; 2009.
- Rubia K, Russell T, Overmeyer S, Brammer MJ, Bullmore ET, Sharma T, et al. Mapping motor inhibition: conjunctive brain activations across different versions of Go/No-Go and stop tasks. *Neuroimage* 2001; 13: 250–61.
- Salmelin R, Schnitzler A, Schmitz F, Freund H-J. Single word reading in developmental stutterers and fluent speakers. *Brain* 2000; 123: 1184–202.
- Schmahmann JD, Pandya D. Fiber pathways of the brain. Oxford: Oxford University Press; 2009.
- Sebastian A, Pohl MF, Klöppel S, Feige B, Lange T, Stahl C, et al. Disentangling common and specific neural subprocesses of response inhibition. *Neuroimage* 2013; 64: 601–15.
- Smith SM, Jenkinson M, Johansen-Berg H, Rueckert D, Nichols TE, Mackay CE, et al. Tract-based spatial statistics: voxelwise analysis of multi-subject diffusion data. *Neuroimage* 2006; 31: 1487–505.
- Sommer M, Koch MA, Paulus W, Weiller C, Büchel C. Disconnection of speech-relevant brain areas in persistent developmental stuttering. *Lancet* 2002; 360: 380–3.
- Talati A, Hirsch J. Functional specialization within the medial frontal gyrus for perceptual Go/No-Go decisions based on ‘what,’ ‘when,’ and ‘where’ related information: an fMRI study. *J Cogn Neurosci* 2005; 17: 981–93.
- Tian X, Zarate JM, Poeppel D. Mental imagery of speech implicates two mechanisms of perceptual reactivation. *Cortex* 2016; 77: 1–12.
- Tourville JA, Reilly KJ, Guenther FH. Neural mechanisms underlying auditory feedback control of speech. *Neuroimage* 2008; 39: 1429–43.
- Toyomura A, Fujii T, Kuriki S. Effect of external auditory pacing on the neural activity of stuttering speakers. *Neuroimage* 2011; 57: 1507–16.
- Turkeltaub PE, Eden GF, Jones KM, Zeffiro TA. Meta-analysis of the functional neuroanatomy of single-word reading: method and validation. *Neuroimage* 2002; 16: 765–80.
- Wakana S, Caprihan A, Panzenboeck MM, Fallon JH, Perry M, Gollub RL, et al. Reproducibility of quantitative tractography methods applied to cerebral white matter. *Neuroimage* 2007; 36: 630–44.
- Watkins KE, Smith SM, Davis S, Howell P. Structural and functional abnormalities of the motor system in developmental stuttering. *Brain* 2008; 131: 50–9.
- Winkler AM, Ridgway GR, Webster MA, Smith SM, Nichols TE. Permutation inference for the general linear model. *Neuroimage* 2014; 92: 381–97.
- Worsley KJ, Evans AC, Marrett S, Neelin P. A three-dimensional statistical analysis for CBF activation studies in human brain. *J Cereb Blood Flow Metab* 1996; 12: 900–18.
- Wymbs NF, Ingham RJ, Ingham JC, Paolini KE, Grafton ST. Individual differences in neural regions functionally related to real and imagined stuttering. *Brain Lang* 2013; 124: 153–64.
- Yairi E, Ambrose N. Epidemiology of stuttering: 21st century advances. *J Fluency Disord* 2013; 38: 66–87.
- Yairi E, Ambrose NG. Early childhood stuttering I: persistency and recovery rates. *J Speech Lang Hear Res* 1999; 42: 1097–12.
- Yaruss JS, Quesal RW. Overall assessment of the speaker’s experience of stuttering (OASES): documenting multiple outcomes in stuttering treatment. *J Fluency Disord* 2006; 31: 90–115.
- Yoo S-S, Lee CU, Choi BG. Human brain mapping of auditory imagery: event-related functional MRI study [Miscellaneous Article]. *Neuroreport* 2001; 12: 3045–9.
- Zheng D, Oka T, Bokura H, Yamaguchi S. The key locus of common response inhibition network for no-go and stop signals. *J Cogn Neurosci* 2008; 20: 1434–42.